INSTITUTE OF PHYSICS PUBLISHING SMART MATERIALS AND STRUCTURES
Smart Mater. Struct. **10** (2001) 786–793 PII: S0964-1726(01)26514-8

Optimal stabilization of indefinite plate buckling problems

J Geoffrey Chase[1] **and Srinivas Bhashyam**[2]

[1] University of Canterbury, Department of Mechanical Engineering, Private Bag 4800, Christchurch, New Zealand
[2] University of Michigan, Department of Mechanical Engineering, Ann Arbor, Michigan, USA

Received 1 November 2000, in final form 9 April 2001
Published 7 August 2001
Online at stacks.iop.org/SMS/10/786

Abstract
Indefinite plate buckling problems arise when the applied load case results in buckling loads which are not all of the same sign. Examples include the important cases of shear buckling and general combinations of tensile and compressive in-plane edge loads. Optimal controllers which actively stabilize these general, indefinite plate buckling problems, by transforming them into a system of definite plate buckling problems, are presented. Important features of this approach include the ability to select the designed closed loop critical buckling load, and to pre-determine what load cases a given controller will stabilize when the exact load combination varies or is unknown. This last result enables the control designer to know exactly, by design, what load combinations will be stabilized. A numerical example is presented where the controllers developed are employed to stabilize multiple, definite and indefinite buckling modes for laminated composite plates similar to aircraft wing skins.

1. Introduction

Linear plate buckling is a mechanical phenomenon wherein the effective flexural stiffness is reduced by the application of compressive, in-plane edge loads or shear loads. The load at which the plate becomes unstable and buckles is called the critical buckling load and is denoted P_{cr}. Similarly, tensile in-plane edge loads effectively increase the flexural stiffness of the plate.

Linear buckling is an important design constraint in many structural systems, particularly when minimum weight is a primary design objective. Laminated composite aircraft wing skins are an example of a plate structure in which linear buckling is the dominant design constraint. In-plane edge loads are applied as a result of the lift forces on the underside of the wings placing the wing skin panels on the top of the wing in compression. Typically, aircraft wing skins are designed for minimum serviceable weight so the ability to actively increase the axial load capacity of these plate structures has the potential to yield an important mass savings. Additional examples might include maritime applications and the shell structures found on missiles and rockets.

Linear buckling can be mathematically modelled using finite element methods by leveraging the fact that when the critical buckling load is reached the total stiffness matrix is singular. This reduction in flexural stiffness results from compressive and shear in-plane, edge loads, and is modelled by an additive geometric stiffness matrix, $\boldsymbol{K}_{\text{G-total}}$, that is proportional to the magnitude of the edge load(s). For general plate buckling problems $\boldsymbol{K}_{\text{G-total}}$ can be defined as follows:

$$\boldsymbol{K}_{\text{G-total}} = a\boldsymbol{K}_{\text{G}x} + b\boldsymbol{K}_{\text{G}y} + c\boldsymbol{K}_{\text{G}xy} \tag{1}$$

where a, b and c, are real valued scalars that reflect the relative magnitude and direction of the in-plane edge loads in the x, y and shear directions respectively, and the matrices $\boldsymbol{K}_{\text{G}x}$, $\boldsymbol{K}_{\text{G}y}$, and $\boldsymbol{K}_{\text{G}xy}$ are the associated geometric stiffness matrices.

The resulting total stiffness is then given by

$$\begin{aligned}\boldsymbol{K}_{\text{total}} &= \boldsymbol{K} - \lambda * (a\boldsymbol{K}_{\text{G}x} + b\boldsymbol{K}_{\text{G}y} + c\boldsymbol{K}_{\text{G}xy}) \\ &= \boldsymbol{K} - \lambda * \boldsymbol{K}_{\text{G-total}}\end{aligned} \tag{2}$$

where λ is a positive scalar representing the load magnitude. Positive values of a, b and c imply compressive loads or shear loads in the positive direction according to the sign convention employed. Negative values imply tensile axial edge loads or negative shear loads.

When the critical buckling load in a given direction is reached, the total stiffness matrix becomes singular and the

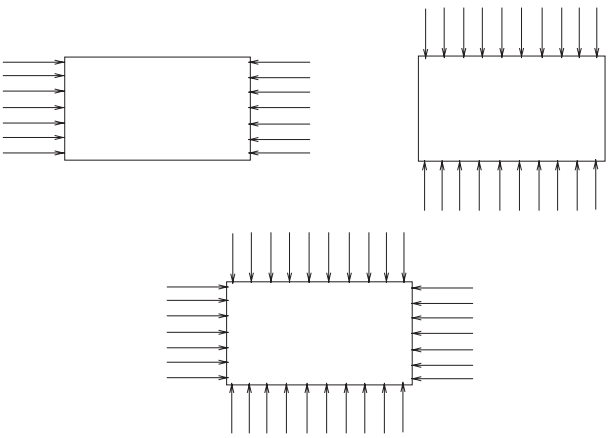

Figure 1. Definite plate buckling load cases.

resulting non-empty nullspace contains a non-zero deflection vector that mathematically satisfies static mechanics with zero applied force (e.g. $K_{\text{total}}v = 0$). Therefore, the critical buckling loads, for a given load case, can be determined via an eigenvalue problem of the form

$$[\boldsymbol{K} - P\boldsymbol{K}_{\text{G-total}}]\bar{v} = \boldsymbol{0} \tag{3}$$

where $\boldsymbol{K}$ is the flexural stiffness matrix, $\boldsymbol{K}_{\text{G-total}}$ is the total symmetric, geometric stiffness matrix, P the eigenvalue, and $\bar{v}$ the eigenvector.

When $P = P_{\text{cr}}$, the plate is unstable in the straight ($\bar{v} = \boldsymbol{0}$) position and any non-zero perturbation will cause it to take on the buckled mode shape. Such perturbations exist naturally in the form of natural curvature, eccentric loading, material non-linearities and residual strains. Therefore, when the critical buckling load is reached for a given load case, the plate will buckle.

Definite plate buckling problems arise when the edge loads are compressive and no shear loads exist ($a, b \geqslant 0$, $c = 0$) as shown in figure 1. The resulting buckling loads are all of the same sign. The problem is definite in that for $\lambda < P_{\text{cr}}$ in equation (2), $\boldsymbol{K}_{\text{total}}$ is positive definite (i.e. all the buckling loads are positive). This fact enables the formulation of positive definite linear matrix inequality (LMI) constraints, employing conditions based on equations (2) and (3), to create stabilizing controllers using semi-definite programming (SDP) techniques (Vandenberghe and Boyd 1995). This approach was utilized in prior optimal buckling control research by Chase *et al* (1999a, b).

Indefinite plate buckling problems do not have buckling loads that are all of the same sign. In the shear buckling case, for which $a = b = 0$ and $c = 1.0$, equation (2) is singular for λ that are distributed symmetrically such that $\lambda = \pm\lambda_i$ for $i = 1, \ldots, (n/2)$. This distribution of positive and negative values of P_{cr}, for the shear buckling case, occurs because the plate buckles due to shear loading of a given magnitude regardless of the direction the load is applied. Figure 2 shows a shear load case. As a result $\boldsymbol{K}_{\text{total}}$ is not positive definite for values of λ near the magnitude of the smallest critical buckling loads. Hence, positive definite conditions cannot be created and SDP cannot be directly applied to these problems.

Indefinite problems also arise when axial edge loads are applied in compressive and tensile combinations as shown in figure 2. Tensile and compressive combinations of axial edge loads result in a total stiffness for which $c = 0$ and the values of a and b are of opposing sign in equation (2). However, the fact that a and b are of opposing signs means that $\boldsymbol{K}_{\text{total}}$ will have both positive and negative valued critical buckling loads in equation (3). Finally, general combinations of shear loading and tensile and compressive axial edge loads will also result in indefinite buckling problems.

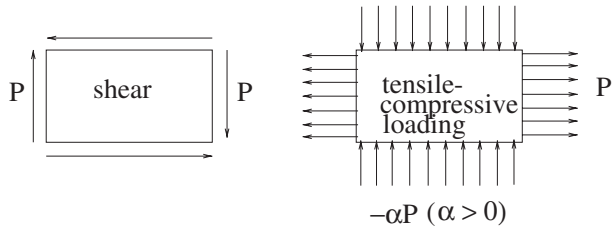

Figure 2. Indefinite plate buckling load case(s).

The lack of specific knowledge about the relative magnitude of multiple, in-plane, edge loads is an important factor that must be accounted for in the design of controllers for structural instability. While the different loads a plate undergoes may be known their relative magnitudes may vary during operation. That variation may be unknown or relatively random so a control design method must be developed that accounts for these variations and enables the designer to understand what load combinations will be stabilized, by design.

For indefinite problems it is impossible to directly create a positive definite LMI, as was done in the definite case. This paper presents two important results for the problem of stabilizing indefinite, general buckling problems. The first is a modified set of optimal design equations that enable the design of optimal buckling controllers for these cases. More specifically, unsolvable indefinite problems are transformed into systems, or series, of definite problems, generalizing and building on results in definite plate buckling control design. The second result is a means of determining what load combinations a controller, designed for multiple load cases, can stabilize. This final result is particularly useful when the exact values of a, b and c are unknown, or vary, for different load cases.

There are few prior results in the area of buckling control, or active strengthening, of plates. Chandrashekara and Bhatia (1993) focused on the finite element analysis of piezo-ceramic actuated buckling plates for definite problems. Definite plate buckling problems were also the focus of the optimal plate buckling controllers developed by Chase and Bhashyam (1999a) in which significant additional results addressed additional issues related to characterizing and overcoming specific architectural and computational difficulties. The majority of the prior research on the stabilization of buckling has been performed for one-dimensional structures such as columns (Berlin 1994, Meressi and Paden 1992, Baz and Tampe 1989, Thompson and Loughlan 1995, Chase *et al* 1997, 1999b, and Berlin *et al* 1998).

The research presented here contains the first results in the area of optimal stabilization of indefinite plate buckling, and are the first application of LMIs and SDP to general, indefinite matrix optimization problems. The following

sections present a short derivation of the optimal design equations and other theoretical results, numerical examples and a set of conclusions.

2. Controller design

Mathematically, the goal is to design an optimal, multi-input, multi-output (MIMO) feedback controller which increases the critical buckling load of a flat plate modelled in the following linear state space form

$$\dot{\boldsymbol{x}}(t) = \boldsymbol{A}(P)\boldsymbol{x}(t) + \boldsymbol{B}_1\boldsymbol{u}(t) \tag{4}$$

where $\boldsymbol{x}(t)$ is the state vector of structural displacements, $\boldsymbol{v}$, and velocities, $\dot{\boldsymbol{v}}$, such that $\boldsymbol{x}(t) = [\boldsymbol{v}^{\mathrm{T}}\ \dot{\boldsymbol{v}}^{\mathrm{T}}]^{\mathrm{T}}$, $\boldsymbol{A}(P)$ is the plant matrix varying as a function of the edge load(s) P, and $\boldsymbol{B}_1$ maps the control inputs $\boldsymbol{u}(t)$ to the appropriate state equation.

The foundation of the control design method presented is the eigenvalue problem of equation (3) and the total stiffness defined in equation (2). Using a finite element model and equation (2) the matrices that define the state space in equation (4) can be created. The plant matrix $\boldsymbol{A}(P)$ and mapping matrix $\boldsymbol{B}_1$ are defined as follows:

$$\begin{aligned} \boldsymbol{A}(P) &= \begin{bmatrix} \boldsymbol{0} & \boldsymbol{I} \\ -\boldsymbol{M}^{-1}\boldsymbol{K}_{\text{total}} & -\boldsymbol{M}^{-1}\boldsymbol{C} \end{bmatrix} \\ \boldsymbol{B}_1 &= \begin{bmatrix} \boldsymbol{0} \\ \boldsymbol{M}^{-1}\boldsymbol{D} \end{bmatrix} \end{aligned} \tag{5}$$

where $\boldsymbol{C}$ and $\boldsymbol{M}$ are the structural damping and mass matrices respectively, and $\boldsymbol{D}$ maps the control inputs to the actuated degrees of freedom. The lower portion of equation (4), using equation (5) represents the second-order equations of motion for a linear dynamic system.

Using static output feedback the control inputs, $\boldsymbol{u}(t)$, can be defined as follows:

$$\boldsymbol{u}(t) = -\boldsymbol{G}\boldsymbol{y}(t) = -\boldsymbol{G}\boldsymbol{C}_1\boldsymbol{x}(t) \tag{6}$$

where $\boldsymbol{y}(t)$ is the vector of measured outputs, defined $\boldsymbol{y}(t) = \boldsymbol{C}_1\boldsymbol{x}(t)$, and $\boldsymbol{G}$ is the gain matrix. This definition of $\boldsymbol{y}(t)$ assumes that displacement and/or velocity measurements are available, but, can easily be generalized for more general forms such as acceleration feedback. Assuming that $\boldsymbol{C}_1 = \mathrm{diag}(\boldsymbol{C}_{1:11}\ \boldsymbol{C}_{1:22})$ is block diagonal and that $\boldsymbol{G} = [\boldsymbol{G}_1\ \boldsymbol{G}_2]$ are conformable blocks, then following the derivation in Chase and Bhashyam (1999a) results in the multi-objective optimization problem used to create optimal controllers for the definite plate buckling problem:

$$\begin{aligned} \min\quad & \alpha P + \beta\lambda_{\mathrm{c}} + \gamma\theta \\ \text{subject to}\quad & \bar{\Phi}^{\mathrm{T}}[(\boldsymbol{K} + \boldsymbol{D}\boldsymbol{G}_1\boldsymbol{C}_{1:11}) + P\boldsymbol{K}_{\text{G-total}}]\bar{\Phi} > \boldsymbol{0} \\ & \bar{\Phi}^{\mathrm{T}}[(\boldsymbol{C} + \boldsymbol{D}\boldsymbol{G}_2\boldsymbol{C}_{1:22}) + \lambda_{\mathrm{c}}\boldsymbol{I}]\bar{\Phi} > \boldsymbol{0} \\ & \begin{bmatrix} \theta\boldsymbol{I}_m & \boldsymbol{G} \\ \boldsymbol{G}^{\mathrm{T}} & \boldsymbol{I}_n \end{bmatrix} \geqslant \boldsymbol{0} \\ & P < -P_{\text{desired}} \end{aligned} \tag{7}$$

where α, β and γ are positive scalars which weight specific terms in the objective function, and the variables λ_{c} and θ are related to constraints on damping and control effort.

The matrix $\bar{\Phi}$ consists of dynamic eigenvectors of the original system which are employed to create an accurate modal representation. This contraction reduces the large optimization problem, that arises from the number of degrees of freedom required to create an accurate modal finite element model, and creates a computationally tractable sized optimization problem. Issues of problem size and computational tractability were reported extensively in Chase and Bhashyam (1999a), and will be eased somewhat by steadily improving computational ability. It is important to ensure that enough dynamic mode shapes are employed, in creating the modal model, to fully describe the resulting closed loop and uncontrolled buckling modes of interest. Finally, it should be noted that the control gains, $\boldsymbol{G}_1$ and $\boldsymbol{G}_2$, remain, and are designed, in the 'physical' domain with no transformation required for actual implementation.

Equation (7) is employed to design optimal controllers with maximum control efficiency by using the the variables $\boldsymbol{G}_1$, $\boldsymbol{G}_2$, P, λ_{c} and θ to modify system stiffness and damping while satisfying the constraint on desired buckling load, P_{desired}. The relative weighting on the objectives trades off the positive value of θ, associated with control effort, with the negative values of P and λ_{c}, associated with increasing the stiffness and damping. The increases in stiffness and damping are accomplished by reversing the sign of the eigenvalues P and λ_{c}, from minus to plus, in the LMI constraints so that minimizing the maximum eigenvalue has the effect of maximizing the minimum eigenvalue of the original eigenvalue problem. As a result, for definite problems, P and λ_{c} are negative valued rather than positive. An important feature of this problem is its convexity which implies that the optimal solution is a unique global minima, and therefore an infeasible result serves as a proof that no solution exists.

However, as noted previously, the positive definite LMI constraints in equation (7) are not valid for indefinite problems. In particular, with buckling loads of both signs, it is not possible to directly modify the minimum magnitude eigenvalues that represent the critical buckling loads at which the plate first buckles. The primary result of this paper is the transformation of equation (7) to create a system of positive definite LMI constraints for which the minimum magnitude eigenvalues are the eigenvalues optimized, as in the definite problem.

Indefinite problems are characterized by having both positive and negative buckling loads (eigenvalues), rather than having all the buckling loads (eigenvalues) of the same sign. Therefore, the transformation to a definite problem from an indefinite problem can be based on separating the two sets of eigenvalues and optimizing them simultaneously over the same control gain variables. Separation is accomplished by using the complete set of buckling eigenvectors, $\boldsymbol{V}$, and partitioning them into separate matrices, $\boldsymbol{V} = [\boldsymbol{V}_+\ \boldsymbol{V}_-]$, associated with the positive, $\boldsymbol{V}_+$, and negative, $\boldsymbol{V}_-$, buckling loads. These matrices are used to contract the LMIs in equation (7) into portions associated with the positive and negative eigenvalues. It is important to note that $\boldsymbol{V}_+$ and $\boldsymbol{V}_-$ are obtained from the contracted model if the matrix $\bar{\Phi}$ is employed, as in equation (7), and directly from the physical system model if $\bar{\Phi}$ is not used. With this approach, $\boldsymbol{V}_+$ and $\boldsymbol{V}_-$ will be conformable.

To create the same definite LMI constraints which allow the minimum magnitude eigenvalues to be modified directly,

the sign of the geometric stiffness term associated with the negative valued eigenvalues must be changed from plus back to minus. The modified optimal control design equations are then defined:

$$\begin{aligned}
&\min \qquad \alpha_+ P_+ + \alpha_- P_- + \beta\lambda_c + \gamma\theta \\
&\text{subject to} \\
&\boldsymbol{V}_+^{\mathrm{T}}\bar{\Phi}^{\mathrm{T}}[(\boldsymbol{K} + \boldsymbol{D}\boldsymbol{G}_1\boldsymbol{C}_{1:11}) + P_+\boldsymbol{K}_{\text{G-total}}]\bar{\Phi}\boldsymbol{V}_+ > \boldsymbol{0} \\
&\boldsymbol{V}_-^{\mathrm{T}}\bar{\Phi}^{\mathrm{T}}[(\boldsymbol{K} + \boldsymbol{D}\boldsymbol{G}_1\boldsymbol{C}_{1:11}) - P_-\boldsymbol{K}_{\text{G-total}}]\bar{\Phi}\boldsymbol{V}_- > \boldsymbol{0} \\
&\bar{\Phi}^{\mathrm{T}}[(\boldsymbol{C} + \boldsymbol{D}\boldsymbol{G}_2\boldsymbol{C}_{1:22}) + \lambda_c\boldsymbol{I}]\bar{\Phi} > \boldsymbol{0} \\
&\begin{bmatrix} \theta\boldsymbol{I}_m & \boldsymbol{G} \\ \boldsymbol{G}^{\mathrm{T}} & \boldsymbol{I}_n \end{bmatrix} \geqslant \boldsymbol{0} \\
&P_+ < -P^+_{\text{desired}} \\
&P_- < -P^-_{\text{desired}}
\end{aligned} \tag{8}$$

where P_+ and P_- are the eigenvalues associated with the positive and negative valued buckling loads and P^+_{desired} and P^-_{desired} are the associated desired buckling loads. Note the different sign for the geometric stiffness term between the two LMI constraints. For a shear buckling problem $P^+_{\text{desired}} = P^-_{\text{desired}}$, as the designer is effectively optimizing symmetric load cases separately. Finally, the damping LMI constraint is unchanged as is the constraint on control effort since these portions of the problem were definite.

In essence, by breaking the problem into portions associated with positive and negative eigenvalues the definiteness of the problem is restored. With definite problems, modification of the minimum magnitude buckling load (eigenvalue) is straightforward because the eigenvalue problem can be formulated such that the minimum magnitude buckling load (eigenvalue) is the maximum eigenvalue by reversing the sign of the geometric stiffness term. This transformation enables the design of controllers which modify the minimum magnitude eigenvalues which were neither the maximum, or the minimum, eigenvalues in the original indefinite problem. Overall, this convex optimization problem is effectively the same as equation (7).

Similar to the definite buckling control design problem the tradeoff between control effort and performance is done in the objective function. By selecting the desired buckling loads explicitly, specific performance is not undefined and they therefore provide a fixed value around which a control effort efficient controller may be designed. Thus, the problem is fully constrained without being over-restricted.

Finally, quadratic stability of the closed loop system can be considered either directly in the control design problem, or as a separate analysis. Considering stability in the design requires an additional LMI constraint considering the standard closed loop Lyapunov equation. However, the additional variables associated with the Lyapunov matrix can make this approach computationally prohibitive. This research considers quadratic Lyapunov stability as a separate problem, checking dynamic stability of the closed loop system after the control gains are designed, rather than concurrently.

3. Stabilization of unknown load cases

For many practical problems the exact values of a, b, c in equation (2), which define the exact load case, may not be known. If these values are known they are easily substituted into equation (8), however, if they are unknown, or vary, equation (8) may not be directly useful. The following discussion presents a modified method of control design, and a means of determining what combinations of load cases can be stabilized by a controller concurrently designed for multiple, individual load cases. More specifically, the method presented shows how concurrent control design for individual load cases can be used to stabilize combined multi-load cases with specific, calculable closed loop critical buckling loads.

To begin this discussion, assume that two *definite* LMI constraints are concurrently applied, in equation (7), creating a set of optimal control gains $\boldsymbol{G}$, for which the following inequalities are valid over the range of P_x and P_y specified:

$$\begin{aligned}
&\bar{\Phi}^{\mathrm{T}}[(\boldsymbol{K} + \boldsymbol{D}\boldsymbol{G}_1\boldsymbol{C}_{1:11}) + P_x\boldsymbol{K}_{\mathrm{G}x}]\bar{\Phi} > \boldsymbol{0} \\
&\qquad \forall -P_x < P^x_{\text{desired}} \\
&\bar{\Phi}^{\mathrm{T}}[(\boldsymbol{K} + \boldsymbol{D}\boldsymbol{G}_1\boldsymbol{C}_{1:11}) + P_y\boldsymbol{K}_{\mathrm{G}y}]\bar{\Phi} > \boldsymbol{0} \\
&\qquad \forall -P_y < P^y_{\text{desired}}
\end{aligned} \tag{9}$$

where P_x and P_y are the variables for the critical buckling loads for compressive edge loads in the 'x' and 'y' directions, respectively. Employing these two constraints results in a set of control gains $\boldsymbol{G}$ which stabilizes either compressive edge loads in the 'x' or 'y' directions to specified values of P^x_{desired} and P^y_{desired}. Note that these constraints do not account for simultaneous 'x' and 'y' direction loading. Equation (9) can be rewritten, using strict inequalities, in standard eigenvalue form to create the following two conditions for the closed loop system:

$$\begin{aligned}
&\bar{\Phi}^{\mathrm{T}}[(\boldsymbol{K} + \boldsymbol{D}\boldsymbol{G}_1\boldsymbol{C}_{1:11}) - P_x\boldsymbol{K}_{\mathrm{G}x}]\bar{\Phi} > \boldsymbol{0} \qquad \forall P_x < P^x_{\text{desired}} \\
&\bar{\Phi}^{\mathrm{T}}[(\boldsymbol{K} + \boldsymbol{D}\boldsymbol{G}_1\boldsymbol{C}_{1:11}) - P_y\boldsymbol{K}_{\mathrm{G}y}]\bar{\Phi} > \boldsymbol{0} \qquad \forall P_y < P^y_{\text{desired}}
\end{aligned} \tag{10}$$

where the signs have been switched to represent a standard formulation of the buckling eigenvalue problem. Equations (9) and (10) are equivalent statements.

The only proven result from equation (9) is that either of these edge loads will be independently stabilized up to the desired limit in compression and for any value in tension. The important question is, over what range of a scalar, $\xi \in [0,\ 1]$, is the following statement valid?

$$\begin{aligned}
&\bar{\Phi}^{\mathrm{T}}[(\boldsymbol{K} + \boldsymbol{D}\boldsymbol{G}_1\boldsymbol{C}_{1:11}) - \xi P^x_{\text{desired}}\boldsymbol{K}_{\mathrm{G}x} - (1-\xi) \\
&\quad \times P^y_{\text{desired}}\boldsymbol{K}_{\mathrm{G}y}]\bar{\Phi} > \boldsymbol{0}
\end{aligned} \tag{11}$$

where this equation asks over what range of convex load combinations is the plate stabilized, given that equation (10) is true?

When $\xi = 1$ or 0, equation (11) degenerates to one or the other portion of equation (10) and the statements validity is obvious. For $0 < \xi < 1.0$ equation (11) can be rewritten as follows:

$$\begin{aligned}
&\bar{\Phi}^{\mathrm{T}}[\xi\{(\boldsymbol{K} + \boldsymbol{D}\boldsymbol{G}_1\boldsymbol{C}_{1:11}) - P^x_{\text{desired}}\boldsymbol{K}_{\mathrm{G}x}\} \\
&\quad +(1-\xi)\{(\boldsymbol{K} + \boldsymbol{D}\boldsymbol{G}_1\boldsymbol{C}_{1:11}) - P^y_{\text{desired}}\boldsymbol{K}_{\mathrm{G}y}\}]\bar{\Phi} > \boldsymbol{0}
\end{aligned} \tag{12}$$

where both terms in the equation are positive definite, and the validity of this equation for $\xi \in (0,\ 1)$ is shown by equation (10). Note that if one of the edge loads

is a tension rather than compression load the sign of the associated geometric stiffness term switches and that portion of equation (12) is still valid.

Hence, if an optimal controller is simultaneously designed for two separate, definite, compressive load cases, then it will also stabilize all convex combinations of those load cases, as well as combinations involving tension of either of the applied loads, to the desired critical buckling loads. This control design method effectively stabilizes an infinite number of load cases that involve the specified edge loads by stabilizing all convex combinations of those edge loads. In essence, a user-specified bound on the acceptable load combinations is provided by this formulation, a valuable design tool when relative loading varies or is unknown.

Since this result is valid for convex combinations of tensile and compressive loads the associated indefinite problem(s) may be stabilized by the simultaneous solution of two definite problems. Specifically, if the 'x' direction is loaded in compression and the 'y' in tension then as long as the magnitude of the compression load does not exceed the magnitude of its designed load (P^x_{desired}) the plate will remain stable. The same statement will be true if the directions of the loads are switched.

Finally, the preceding arguments are easily generalized to include shear load cases as well as compressive and tensile edge loads. Each load case must have its own LMI constraint in the optimal equations in the form of equation (7) or (8), depending on whether it is a definite or indefinite load case. For example, if shear loads are included, the control design equations must include constraints similar to those used in equation (8) because the shear problem is indefinite by definition. Therefore, rather than trying to specify the specific load balance among multiple loads the overall, optimal control design equation simply includes LMI constraints for each load case individually, each with their own desired value of $P_{\text{cr}} = P_{\text{desired}}$. This approach provides the greatest design flexibility to the designer offering variable choices of closed loop critical buckling load for each edge load and stabilizing all convex combinations of those loads.

In summary, this section presents a way of solving indefinite problems involving in-plane tensile and compressive load combinations by solving two definite problems, generalizing and building on prior results in this area. This approach to control design is also shown to enable the determination of what load combinations a controller designed for multiple independent load cases can stabilize. Hence, it is suggested that the best design method for cases where the exact load combination is unknown, or varies, is the simultaneous design of controllers for each individual expected load. In this fashion, values of P_{desired} for each direction can be chosen, using the analysis methods presented, so that the range of expected load combinations will be stabilized.

4. Numerical verification

This section presents a brief numerical example that verifies the optimal control design methods presented for a shear buckling problem. The determination of what loads are stabilized for multiple load case combinations is also investigated.

The specific problem is the stabilization of a square plate measuring 20.3 cms on a side. The plate is clamped on all four sides and is made of a graphite epoxy laminated composite similar to those found in aircraft wing skins. The overall goal of adding active control to this stabilize aircraft wing skins is to save weight, using active elements to stabilize thinner or larger plates, reducing the total structural weight of the wing structure in the process. The resulting plate has an approximate thickness of 0.25 cms with a ply layup of:

$$[\pm 45, 90, -45, 90, 45, 90, 45, 90, -45, 90, -45, 0, 45, 0, -45]_S \tag{13}$$

where the values are angles in degrees and the subscript $\boldsymbol{S}$ denotes a symmetric layout of the 16 plies shown. This ply layup results in specially orthotropic material behaviour and a flexural modulus, $\boldsymbol{D}_{ij}$, of the following form:

$$\boldsymbol{D}_{ij} = \begin{bmatrix} 32\,100 & 23\,623 & -9.04 \\ 23\,623 & 84\,004 & -9.04 \\ -9.04 & -9.04 & 26\,246 \end{bmatrix} \text{ (N cm)}. \tag{14}$$

It is important to note that the design approach presented will work for any type of plate, not just laminated composites or specially orthotropic materials. The goal of this numerical example is to show the validity of the control method presented and its ability to handle multiple load cases as per the discussion in previous sections. Specially orthotropic materials are used as this aircraft wing skin example shows a positive tradeoff benefit in terms of weight savings as per the results from Chase and Bhashyam (1999a). The method presented does not directly handle anisotropic laminated composite plates that often contain significant residual strains due to their asymmetric ply layup. These cases will only work effectively if the finite element model used for control design accounts for these residual strains. Hence, this method is valid for any system for which linear finite element modelling provides good correlation of the structural instability.

The plate is modelled by a finite element model employing 64 elements with 4 degrees of freedom per node and 196 total degrees of freedom for the plate. Each element is approximately 2.54 cm on a side and the finite element models employed for analysing buckling loads were derived as per the work by Shames and Dym (1996). Finite element results are correlated using the analytical results presented by Shames and Dym (1996) and Young (1989).

For axial loading the correlation between finite element loads and analytical results were very good. The open loop, uncontrolled, critical buckling load in the along the 'x' and 'y' axes, $P^x_{\text{cr}} = P^y_{\text{cr}}$, were within 0.25% of analytical results. Correlation of the shear critical buckling load, P^{xy}_{cr}, was within 5.7% of the analytical prediction. This lower correlation, while marginal, would be improved to less than 1% by using a larger number of elements per side, such as 12 or 16, rather than the eight employed. The 8×8 model was still employed to minimize computational intensity and prove the concept. Correlation of natural frequencies was within 0.03% of analytical results and static analysis of the models using uniform pressure loads delivered displacements within 0.025% of analytical results for this 8×8 model. Overall, analytical correlation was excellent and the differences in shear loading results were seen as acceptable to maintain a direct

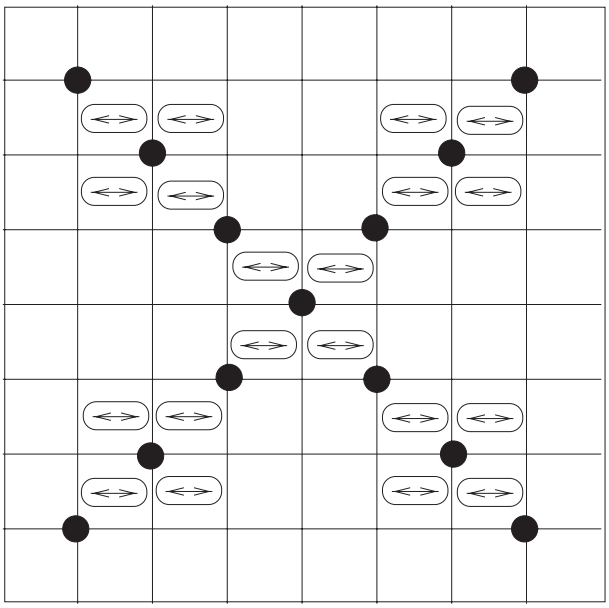

Figure 3. Control architecture for the active plate.

comparison with previously reported results and for a proof of concept verification, particularly given the otherwise excellent correlation with analytical results.

Sensing and actuation comprise the essential elements of a control system architecture and are modelled as specifically oriented patches of piezoceramic filaments and MEMS strain sensors with a precision of 5 $\mu\epsilon$. The sensors are assumed to be laid out in a quantity such that lateral deflections can be accurately estimated at desired locations from these strain measurements. The peak moment a pair of the piezoceramic actuator patches, located on either side of the plate, can generate is $M_{\max} = 81.4$ N cm. This induced moment is oriented about the in-plane axis perpendicular to the orientation of the piezoceramic filaments. The sensors and actuators modelled are based on the experimental equipment employed in Chase *et al* (1999b).

The exact control architecture is given in figure 3 where the black dots represent points at which lateral deflection is estimated and the arrows indicate an element covered with a filament piezoceramic patch oriented in the direction shown. Each actuated element, with an oval, represents an individual control input, so that this problem has 20 control inputs and 13 measurements (26 including velocity measurements). The resulting control gain matrix, $\boldsymbol{G}$, is therefore of size (20×26).

This control architecture is identical to that employed for definite axial buckling load cases in Chase and Bhashyam (1999a) and is employed here for consistency. This architecture was selected to provide a positive mass tradeoff when an active system was employed, saving aircraft mass, a critical constraint for high performance aircraft. The specific choice of measurements and architecture employed were selected after a great deal of trial and error.

The identical control architecture is employed to show that it is equally applicable for indefinite, as well as multiple, buckling load cases and to provide a comparison to the simpler, definite buckling stabilization case. The prior result, for definite axial load cases, also provides a further result for verification as the indefinite case, at its simplest, is simply broken into multiple definite cases. Hence, the design methodology and verification example are consistent across these two cases enabling more in-depth comparison of the results obtained.

The specific multiple buckling load case chosen combines a definite axial buckling load in the 'x' direction with a pure shear buckling load. This combination reflects the compressive axial loading seen by an aircraft wing skin with the shear loading that can arise due to external loads applied during aircraft turns. Additionally, these loads are a combination of an indefinite buckling load case and the definite load case originally reported (Chase and Bhashyam 1999a).

Optimal control gains are simultaneously designed for both the pure shear load case and for the compressive loads in the 'x' direction. Definite LMI constraints of the form used in equation (8) are used to design control gains for the shear loads, and LMIs for definite problems, as in equation (7), are employed for the definite axial load case. The specific optimal equation, which combines these two constraint sets to be satisfied concurrently, is given as follows:

$$\begin{aligned}
\min \quad & \alpha P_x + \alpha_+ P_+ + \alpha_- P_- + \beta\lambda_c + \gamma\theta \\
\text{subject to} \quad & \bar{\Phi}^{\mathrm{T}}[(\boldsymbol{K} + \boldsymbol{D}\boldsymbol{G}_1\boldsymbol{C}_{1:11}) + P_x\boldsymbol{K}_{\mathrm{G}x}]\bar{\Phi} > \boldsymbol{0} \\
& \bar{\Phi}^{\mathrm{T}}[(\boldsymbol{C} + \boldsymbol{D}\boldsymbol{G}_2\boldsymbol{C}_{1:22}) + \lambda_c\boldsymbol{I}]\bar{\Phi} > \boldsymbol{0} \\
& \boldsymbol{V}_+^{\mathrm{T}}\bar{\Phi}^{\mathrm{T}}[(\boldsymbol{K} + \boldsymbol{D}\boldsymbol{G}_1\boldsymbol{C}_{1:11}) + P_+\boldsymbol{K}_{\mathrm{G}xy}]\bar{\Phi}\boldsymbol{V}_+ > \boldsymbol{0} \\
& \boldsymbol{V}_-^{\mathrm{T}}\bar{\Phi}^{\mathrm{T}}[(\boldsymbol{K} + \boldsymbol{D}\boldsymbol{G}_1\boldsymbol{C}_{1:11}) - P_-\boldsymbol{K}_{\mathrm{G}xy}]\bar{\Phi}\boldsymbol{V}_- > \boldsymbol{0} \\
& \begin{bmatrix} \theta\boldsymbol{I}_m & \boldsymbol{G} \\ \boldsymbol{G}^{\mathrm{T}} & \boldsymbol{I}_n \end{bmatrix} \geqslant \boldsymbol{0} \\
& P_x < -P^x_{\mathrm{desired}} \\
& P_+ < -P^+_{\mathrm{desired}} \\
& P_- < -P^-_{\mathrm{desired}}
\end{aligned} \tag{15}$$

where all the terms have been defined previously. There is one LMI for the definite, axial buckling load case involving $\boldsymbol{K}_{\mathrm{G}x}$ and P_x and two more for the indefinite pure shear buckling load using $\boldsymbol{K}_{\mathrm{G}xy}$, P_+ and P_-. There are additional LMIs for the damping, velocity feedback, gains, control effort θ and the desired buckling load constraints. Additionally, there are now far more parametric combinations in the objective function, although they are traded off, as a whole, against control effort θ, as might be expected. Note that this equation is unique to this particular combination of pure axial and shear load cases and must be set up for each combination to be analysed, however, the solution and application of the finite element models and other aspects are entirely the same.

Each load case employs a value of $P_{\mathrm{desired}} = 1.5P_{\mathrm{cr}}$ for designing the control gains. The design results are presented in table 1 where the uncontrolled, desired, and closed loop values are given for the buckling loads in the axial and shear directions. In addition, the value of θ, the maximum singular value of the control gains $\boldsymbol{G}$ is presented.

In this case, it is apparent that the shear load case is driving the design. Table 1 shows the closed loop critical buckling load for the shear case is tight against it is constraint while it is loose for the axial load case. This result is due to the specific control architecture employed and the inability to increase the shear load, without increasing the axial load, using

Table 1. Results for optimal control gains concurrently designed for axial and shear loads.

	Axial P_{cr} (N cm^{-1})	Shear P_{cr} (N cm^{-1})	θ
Open loop	12 728	22 192	—
Desired	19 079	33 287	—
Closed loop	24 321	33 287	7.7e+7

Table 2. Results for optimal control gains for axial load only.

	Axial P_{cr} (N cm^{-1})	θ
Open loop	12 728	—
Desired	19 079	—
Closed loop	24 321	2.4e+7

this architecture. A significantly different control architecture, explicitly designed for controlling shear loads, would have had a more efficient result.

For comparison an optimal controller was designed for the axial load case alone, using the same value of P^x_{desired}, for which the results are shown in table 2. The result of $\theta = 2.4\text{e} + 7$ illustrates the effect of the additional constraints for stabilizing the shear load case. Note that this value of θ is one third the size of the value of θ obtained in concurrently designing the control gains for both shear and axial loads.

It is clear from this comparison how important the control architecture is to the efficiency and ability to control the structural instability. This study also confirmed earlier results that show the active elements act like active stiffeners. In plate buckling problems the structure effectively 'squeezes' out between these stiffeners and buckling mode shapes shift to find areas of lesser resistance. In this example, while the architecture was not perfectly efficient for the axial load alone it was less efficient in combination with the shear buckling case. Hence, as seen in table 1, the shear load is tight against the constraint, as it is the driving factor in the optimization, and the final closed loop axial critical buckling load is far higher than the desired value.

The excess effective strength in the axial direction comes at the cost of more expensive control. It is important to note that this result is not necessarily bad and that the magnitudes of the load combinations that may be stabilized with the resulting control gains are increased by the higher resulting closed loop axial buckling load. Finally, as the number of measurements and control inputs rises the control efficiency of the resulting control design increases as well since the ability to handle multiple modes goes up with the increasing resolution of the control inputs with respect to the shape of the buckling modes to be stabilized.

To see if the resulting closed loop system was stable for a variety of possible load combinations, several convex combinations of these two load cases were tested. These analyses were performed to verify the contention of equations (12) and (15), that the concurrent solution of control gains for multiple load cases, in this case axial and shear loads, will stabilize not only those load cases but any convex combination of the resulting closed loop critical buckling loads for those cases. Hence, if the closed loop axial and shear critical buckling loads were applied in some convex combination, using equation (11), these analyses are used to confirm that the system is stabilized as expected.

To test this contention several convex combinations of the closed loop critical buckling loads from table 1 were selected and the closed loop plant matrix constructed for these loads at the boundary. The eigenvalues were then calculated using Matlab to determine if there were one or more roots effectively on the imaginary axis (borderline stable) with the remaining roots located in the left-hand side of the complex plane (stable). Lower values, in the fully stabilized region, were run to ensure stability there as well. These analyses are not intended to be exhaustive but rather to 'physically' check the proof in the mathematics leading to equation (12) and the design method presented.

In each case the the closed loop plant was stable verifying the analysis in the prior section. Simulations were also run for some of these cases to confirm the eigenvalue analysis results. In this fashion, the controllers designed are validated for a number of load combinations rather than a single individual load case or a given load combination. This result illustrates the power of this approach to optimal control design for cases in which the exact load combination is unknown. In particular, it is seen that one control design can cover, or bound, a number of load cases, simply and effectively handling a major uncertainty in the design of controllers for structural instability.

Finally, simulations were performed to test the controllers. The individual axial and shear load cases were simulated separately to determine the maximum initial displacement, in the shape of the first buckling mode, that could be stabilized for each load case. These simulations effectively test the individual load cases for stability and present a means of obtaining extreme initial conditions for any combined load cases. Note that while the structural instability is stabilized by a given control design if the initial deflection and/or velocity exceeds the actuator authority of the system it will be unable to bring the structure back to it is initial, undeformed shape. This type of failure is a function of actuator authority and sensor precision. Stronger actuators enable the system to be stabilized from greater initial conditions, while greater sensor resolution and bandwidth enables the system to respond faster to smaller excursions from the nominal.

A robustness ratio is presented to measure, using simulation results, the effectiveness of the control architecture elements selected. This ratio compares the maximum initial deflection that may be stabilized to the minimum deflection that the sensors can measure. The sensors assumed for this study have a resolution of 5 $\mu\epsilon$ at a bandwidth of 1000 Hz. The simulations were performed using this sensor resolution and controller bandwidth with the peak actuation force for the piezoceramic filament actuators as given previously.

Table 3 provides the robustness ratios for the axial and shear cases alone as well as the 50–50 convex combination. These results are fairly constant with a value of just over 8.0 for each case, similar to prior results for plates this stiff, using MEMS-based actuators and sensors. Note that the axial case robustness ratio is slightly lower than reported for the axial case alone due to the different control gains obtained for the multiple load case problem presented here. Of particular note is the idea that if sensor resolution were improved to 1 $\mu\epsilon$ and actuator authority were increased by a factor of 5x, then

Table 3. Robustness ratios for different load cases.

	Robustness ratio
Axial alone	8.70
Axial	8.40
Shear	8.65
50–50 comb.	8.55

the robustness ratio would go up by as many as two orders of magnitude (Chase and Bhashyam 1999a).

This last result is important since a robustness ratio of 8 along with minimum detectable deflections of 0.0019 mm for the axial buckling mode and 0.016 mm for the shear buckling mode, implies that the maximum initial deflection that may be stabilized is between 0.015 and 0.13E−1 mm. These values are very small and may occur simply as a function of eccentric loading or natural curvature of the composite plate. A more realistic implementation would have a robustness ratio of at least 100–200 to ensure more realistic, stabilizable displacements for this implementation on the order of 5.00 mm or larger.

In each of these simulations the individual buckling loads are set at at an appropriate convex combination of the original $1.3P_{cr}$ loads used to simulate each individual load case. This value is very near the design limit that was set at $1.5P_{cr}$ in the optimization problem. For each of the convex load combinations tested, the controller was able to stabilize initial deflections eight times, or more, the size of the minimum deflection detectable with the strain sensors.

This last result serves to verify the two main results of this research. First, that the approach presented for designing controllers for indefinite buckling problems, as a combination of concurrently solved definite plate buckling control problems, is feasible and practicable. Secondly, and far more importantly, that concurrently stabilizing multiple load cases also stabilizes the convex combinations of those loads, bounding, by user specified constraint, the stabilizable range of load combinations for the system. This last result is the most important as many applications do not undergo constant uniform loading and instead are designed with significant uncertainty regarding relative load magnitudes.

5. Conclusions

This research investigates the design and implementation of optimal buckling controllers for indefinite plate buckling problems. An optimization problem which transforms indefinite problems into a series of solvable definite problems is formulated and represents the first application of linear matrix inequalities and SDP to indefinite matrix optimization problems. The method presented can be generalized to larger classes of indefinite matrix optimization problems.

A method of analysis is also presented which allows the designer to determine the entire range of load combinations that may be stabilized by simultaneously designing a controller for individual load cases. This approach allows certain indefinite problems to be solved as a series of definite control design problems. More importantly, it suggests an effective design method for cases in which the exact load combination is not known, or varies under certain conditions.

The methods developed are verified by the development of optimal buckling controllers for stabilizing plate buckling under shear and other generalized load cases. An optimal controller is designed simultaneously for both an axial (definite) and a shear (indefinite) load case. The control architecture and its impact on control design and the resulting controller are discussed along with the impact of sensor resolution and actuator authority on controlling structural instability. The interaction between the system and the control design are fully discussed for this example to outline the overall design approach necessary for these applications. The resulting controller design is able to stabilize both the individual load cases to the specified desired values, as well as convex combinations of the input load values, verifying the design methods presented. This last result produces a user specified bound on the stabilizable load combinations designed. Overall, it is seen that multi-load case indefinite plate buckling can be readily stabilized, to user specified limits, using the methods presented while simultaneously developing a bound on the stabilizable load combinations.

Acknowledgments

This research was supported by the Defense Advanced Research Projects Agency under contract no DABT63-95-C-0025 and was performed at the Xerox Palo Alto Research Center (PARC) in Palo Alto, CA, while the lead author was a member of the research staff.

References

Baz A and Tampe L 1989 Active control of buckling of flexible beams *Proc. 1989 ASME Design Technical Conf. on Failure Prevention and Reliability (Montreal, Canada, Sept.)* pp 211–8

Berlin A A 1994 Towards intelligent structures: active control of buckling *PhD Thesis* Department of Electrical Engineering and Computer Science, Massachusetts Institute of Technology

Berlin A A, Chase J G, Yim M H, Maclean B J, Olivier M and Jacobsen S C 1998 MEMS-Based control of structural dynamic instability *J. Intell. Mater. Syst. Struct.* **9** 574–86

Chandrashekara K and Bhatia K 1993 Active buckling control of smart composite plates—finite element analysis *Smart Mater. Struct.* **2** 31–9

Chase J G, Yim M H, Berlin A A, Olivier M and Maclean B 1997 Mems-based active stabilization of column buckling *Proc. 1997 Int. Mechanical Engineering Congress and Exposition (IMECE) (Dallas, Texas, Nov.)* pp 16–21

Chase J G and Bhashyam S 1999a Optimal stabilization of plate buckling *J. Smart Mater. Struct.* **8** 204–11

Chase J G, Yim M H and Berlin A A 1999b Optimal stabilization of column buckling *ASCE J. Eng. Mech.* **125** 987–93

Meressi T and Paden B 1992 Buckling control of a flexible beam using piezoelectric actuators *J. Guidance* **16** 977–80

Shames I H and Dym C L 1996 *Energy and Finite Element Methods in Structural Mechanics* (New York: Taylor and Francis)

Thompson S P and Loughlan J 1995 The active buckling control of some composite column strips using piezoceramic actuators *Compos. Struct.* **32** 59–67

Vandenberghe L and Boyd S P 1995 Primal–Dual potential reduction method for problems involving matrix inequalities *Math. Program.* B **69** 205-36

Young W C 1989 *Roark's Formulas for Stress and Strain* 6th edn (New York: McGraw-Hill)